Journal of Productivity Analysis (2018) 50:139–154
https://doi.org/10.1007/s11123-018-0539-5

Stochastic non-smooth envelopment of data for multi-dimensional output

Julia Schaefer[1] · Marcel Clermont[2]

Published online: 31 October 2018

Abstract
The proposed method of Stochastic Non-smooth Envelopment of Data (StoNED) for measuring efficiency has to date mainly found application in the analysis of production systems which have exactly one output. Therefore, the objective of this paper is to examine the applicability of StoNED when a ray production function models a production technology with multi-dimensional input and output. In addition to a general analysis of properties required by a ray production function for StoNED to be applicable, we conduct a Monte Carlo simulation in order to evaluate the quality of the frontier and efficiencies estimated by StoNED. The results are compared with those derived via Stochastic Frontier Analysis (SFA) and Data Envelopment Analysis (DEA). We show that StoNED provides competitive estimates in regard to other methods and especially in regard to the real functional form and efficiency.

Keywords Stochastic Non-smooth Envelopment of Data · Ray Production Function · Monte Carlo Simulation · Stochastic Frontier Analysis · Data Envelopment Analysis · Efficiency Analysis

1 Introduction

Stochastic Non-smooth Envelopment of Data (StoNED) is a new method for measuring the efficiencies of decision making units (DMUs). StoNED was developed by Kuosmanen and Kortelainen (2012) and, to date, several economic insights into StoNED have been discussed in the literature and first real-world applications have been conducted (see e.g. Kuosmanen 2012; Kuosmanen et al. 2013; Andor and Hesse 2014; Johnson and Kuosmanen 2015). The main idea behind StoNED is the combination of properties of Data Envelopment Analysis (DEA) with those of Stochastic Frontier Analysis (SFA). Piecewise linear functions are created in an analogous manner to DEA by estimating the production function f (x) with a convex nonparametric least squares regression (CNLS). No particular form of the underlying production function is assumed a priori; it merely has to be continuous, monotonically increasing, and globally concave (Kuosmanen 2008). Additionally, a composite error term, which represents the deviation between the achieved and the maximum possible output, is decomposed analogously to SFA into an inefficiency term and a noise term.

The majority of previous works on StoNED deal with production systems that use several inputs to produce exactly one output. In the real world, however, numerous production systems exist where multiple inputs are used to generate multiple outputs (see e.g. Ahn and Le 2015; Clermont et al. 2015; Jewell 2017). First proposals for measuring the inefficiency of such production systems by StoNED can be found in Kuosmanen et al. (2015a) as well as Kuosmanen and Johnson (2017). Both articles propose a directional distance function to model joint production of multiple outputs.[1] In addition, Kuosmanen and Johnson (2017) develop a new estimator of the directional distance function, which considers axiomatic properties and does not require any assumptions concerning the functional form.

✉ Marcel Clermont
marcel.clermont@dhge.de

[1] School of Business and Economics, Chair of Business Theory, RWTH Aachen University, Templergraben 64, 52056 Aachen, Germany

[2] Duale Hochschule Gera-Eisenach, Am Wartenberg 2, 99817 Eisenach, Germany

[1] A detailed explanation of the basic properties of directional distance functions can be found in Kuosmanen et al. (2015b).

Besides modeling joint productions of multiple outputs by means of a directional distance function, the literature proposes a ray production function (Löthgren 1997). In particular, as an alternative to distance functions, ray production functions are used to enhance SFA analyses for an integration of multiple outputs.[2] Therefore, the question arises of whether modeling multi-dimensional outputs with a ray production function also represents an alternative to directional distance functions for StoNED. We first model the technology by means of a distance function and a ray production function, and demonstrate advantages of ray production functions. Secondly, we show that a ray production function fulfills the required properties in order for StoNED to be applicable.

However, examining the basic applicability does not predict the quality of an efficiency measurement. To perform controlled quality examinations of efficiency measurement methods, Monte Carlo simulations have been established in the literature (see e.g., Badunenko et al. 2012; Resti 2000). Thus, we also conduct a Monte Carlo simulation in order to assess the quality of efficiency measurements by StoNED when using a ray production function to model technologies with multi-dimensional input and output. We analyze the plausibility of the resulting frontiers and efficiencies estimated by StoNED and compare them with those estimated by SFA and DEA, respectively. To address the problem of a potential correlation between the residuals and the explanatory variables in CNLS regression, we additionally investigate the existence of such correlations in the considered scenarios.

The paper is structured as follows: In Section 2, we introduce both an output distance function and a ray production function, and discuss potential merits of a ray production function. Then, we analyze the conditions to justify the applicability of a ray production function for StoNED and present the approach of efficiency measurement by StoNED for production systems with multi-dimensional input and output (Section 3). In Section 4, we present the design of the Monte Carlo simulation and its results. The paper concludes with a summary, a discussion of limitations, and an outlook on further research in Section 5.

[2] Until now, there has been little scientific investigation of the differences that exist between modeling multiple outputs with a directional distant function or a ray production function. For instance, Henningsen et al. (2015) present a Monte Carlo simulation that investigates the qualitative differences between modeling multi-dimensional output with an output distance function and with a ray production function when measuring the efficiency by SFA. In the scenarios considered by their analysis, neither distance function nor ray production function could be shown to be superior to the other.

2 Modeling technologies with multi-dimensional input and output

Below, a DMU is characterized by using a given amount of m different inputs $\boldsymbol{x} = (x_1, \ldots, x_m)^t \in \mathbb{R}^m_{\geq 0}$ to produce a certain amount of s different outputs $\boldsymbol{y} = (y_1, \ldots, y_s)^t \in \mathbb{R}^s_{\geq 0}$. The underlying production technology $\boldsymbol{T}$ can be defined as follows:

$$\boldsymbol{T} = \{(\boldsymbol{x}, \boldsymbol{y}) | \boldsymbol{x} \text{ can produce } \boldsymbol{y}\}. \tag{1}$$

For given input $\boldsymbol{x}$, the production possibility set $\boldsymbol{P}(\boldsymbol{x})$ is given by

$$\boldsymbol{P}(\boldsymbol{x}) = \{\boldsymbol{y} | (\boldsymbol{x}, \boldsymbol{y}) \in \boldsymbol{T}\}. \tag{2}$$

According to Färe and Primont (1995), $\boldsymbol{P}(\boldsymbol{x})$ should fulfill the following three properties:

P1: $\boldsymbol{0} \in \boldsymbol{P}(\boldsymbol{x})\ \forall \boldsymbol{x} \in \mathbb{R}^m_{\geq 0}$

P2: $\boldsymbol{y} \in \boldsymbol{P}(\boldsymbol{x})$ and $0 < \eta \leq 1 \Rightarrow \eta \boldsymbol{y} \in \boldsymbol{P}(\boldsymbol{x})\ \forall \boldsymbol{x} \in \mathbb{R}^m_{\geq 0}$, $\forall \boldsymbol{y} \in \mathbb{R}^s_{\geq 0}$

P3: $\forall \boldsymbol{x} \in \mathbb{R}^m_{\geq 0}$ $\boldsymbol{P}(\boldsymbol{x})$ is a bounded and closed set.

Property P1 ensures that for a given input it is always possible to produce no output ($\boldsymbol{y} = \boldsymbol{0}$). By property P2, the weak disposability of outputs is allowed, i.e. for constant inputs, a proportional reduction of outputs is possible. Property P3 implies that a limited amount of inputs can produce only a limited amount of outputs.

One way of modeling the aforementioned technologies is by using distance functions (Shephard 1953, 1970). In order to demonstrate the principle of the applicability of distance functions, and for simplification purposes, an output distance function is assumed. This can be derived from P2 as follows (Färe and Primont 1995):

$$D_O(\boldsymbol{x}, \boldsymbol{y}) = \inf\left\{\eta | \eta > 0, \frac{\boldsymbol{y}}{\eta} \in \boldsymbol{P}(\boldsymbol{x})\right\}. \tag{3}$$

According to Kumbhakar and Lovell (2003), (3) has the following four properties:

D1: $D_O(\boldsymbol{x}, \boldsymbol{0}) = 0\ \forall \boldsymbol{x} \in \mathbb{R}^m_{\geq 0}$ and $D_O(\boldsymbol{0}, \boldsymbol{y}) = \infty\ \forall \boldsymbol{y} \in \mathbb{R}^s_{>0}$

D2: $D_O(\boldsymbol{x}, \boldsymbol{y}) \leq 1 \Leftrightarrow \boldsymbol{y} \in \boldsymbol{P}(\boldsymbol{x})$

D3: $D_O(x, y) = 1 \Leftrightarrow \boldsymbol{y} \in \text{Isoq}\boldsymbol{P}(\boldsymbol{x}) := \{\boldsymbol{y} | \boldsymbol{y} \in \boldsymbol{P}(\boldsymbol{x}), \lambda \boldsymbol{y} \notin \boldsymbol{P}(\boldsymbol{x}), \lambda > 1\}\ \forall \boldsymbol{y} \in \mathbb{R}^s_{\geq 0}$

D4: $D_O(x, \lambda \mathbf{y}) = \lambda D_O(x, y)\ \forall \lambda > 0$.

D1 basically defines two limiting cases. The first case is when all used inputs are wasted in such a way that no output is generated. Then, the value of the output distance function equals zero. The other case is the production of an output without the use of any inputs; this leads to a function value of infinity. Property D2 indicates an alternative characterization of $\boldsymbol{P}(\boldsymbol{x})$, whereas D3 characterizes the boundary of the production possibility set Isoq$\boldsymbol{P}(\boldsymbol{x})$. Thus, the boundary of the underlying production technology $\boldsymbol{T}$ and the efficient production facilities are described. Property D4 shows that D_O is homogeneous in outputs.

The output distance function can now be used to determine a regression equation with one dependent variable. Given the assumption that the observed DMUs produce only one measured output $y \in \mathbb{R}_{\geq 0}$, the production function $f(\boldsymbol{x})$ is defined as (Löthgren 1997)

$$f(\boldsymbol{x}) = \max\{y \in \mathbb{R}_{\geq 0} | y \in \boldsymbol{P}(\boldsymbol{x})\}. \tag{4}$$

Due to properties D_3 and D_4 $f(\boldsymbol{x})$ can be expressed by

$$f(\boldsymbol{x}) = \frac{1}{D_o(\boldsymbol{x}, 1)}. \tag{5}$$

Based on property D4 the following applies:

$$\begin{aligned} &D_O(\boldsymbol{x}, y) = y \cdot D_O(\boldsymbol{x}, 1) \\ &\quad \Leftrightarrow y = \tfrac{1}{D_O(\boldsymbol{x},1)} \cdot D_O(\boldsymbol{x}, 1). \end{aligned}$$

Because of (5) and $D_O(\boldsymbol{x}, y) = e^{-u}$ (see Kumbhakar/Lovell 2003)

$$y = f(\boldsymbol{x}) \cdot e^{-u} \tag{6}$$

results.

Thus, for any measured output y a positive inefficiency term u is already considered. However, in Eq. (6) measurement errors and approximation errors are part of y. To represent such errors explicitely and to calculate the actual output y, a symmetric noise term v can be included (Coelli et al. 2005):

$$y = f(\boldsymbol{x}) \cdot e^{v-u}. \tag{7}$$

The before mentioned explanations can be carried over to the multi-dimensional measured output $\boldsymbol{y} \in \mathbb{R}^s_{\geq 0}$ case. With

$$f\left(\boldsymbol{x}, \frac{\boldsymbol{y}}{\| \boldsymbol{y} \|}\right) = \max\left\{a \in \mathbb{R}_{\geq 0} | a \cdot \frac{\boldsymbol{y}}{\| \boldsymbol{y} \|} \in \boldsymbol{P}(\boldsymbol{x})\right\} = \frac{1}{D_O\left(\boldsymbol{x}, \frac{\boldsymbol{y}}{\|\boldsymbol{y}\|}\right)} \tag{8}$$

the following holds:

$$\begin{aligned} &D_O\left(\boldsymbol{x}, \tfrac{\boldsymbol{y}}{\|\boldsymbol{y}\|}\right) = \tfrac{1}{\|\boldsymbol{y}\|} D_O(\boldsymbol{x}, \boldsymbol{y}) \\ &\quad \Leftrightarrow \| \boldsymbol{y} \| = \frac{1}{D_O\left(\boldsymbol{x}, \frac{\boldsymbol{y}}{\|\boldsymbol{y}\|}\right)} \cdot D_O(\boldsymbol{x}, \boldsymbol{y}) \\ &\quad \Rightarrow \| \boldsymbol{y} \| = f\left(\boldsymbol{x}, \tfrac{\boldsymbol{y}}{\|\boldsymbol{y}\|}\right) \cdot e^{-u}. \end{aligned} \tag{9}$$

In analogy to (7) the consideration of noise leads to

$$\| \boldsymbol{y} \| = f\left(\boldsymbol{x}, \frac{\boldsymbol{y}}{\| \boldsymbol{y} \|}\right) \cdot e^{v-u}. \tag{10}$$

Equation (10) gives a regression equation that has exactly one dependent variable: the one-dimensional output norm. The inputs and normalized outputs are the regressors in the model. A similar approach was also proposed by Kuosmanen et al. (2015a). Unlike the case of the output distance function shown here, the authors use a directional distance function (Chambers et al. 1996, 1998). Kuosmanen et al. (2015b) show that the directional distance function is a functional representative of the underlying production technology.

The property of homogeneity associated with the definition of the distance function D_O places a restriction on the form of the function to be estimated. A basic principle of StoNED is to keep the properties of the function to be estimated a priori as low as possible, so that the set of potential functions remains as large as possible. The requirement of homogeneity would restrict the appropriate set of possible functions. Furthermore, according to Grosskopf et al. (1997) and Löthgren (2000), the homogeneity property leads to endogeneity problems, which Kuosmanen et al. (2015b) analyze in more detail, with respect to the directional distance function. The preceding points motivate the search for an alternative way to extend StoNED in order to consider multi-dimensional output, namely via a ray production function.

Ray production functions differ from (directional) distance functions in that all possible output combinations in the production possibility set are now mapped by their polar coordinates (Löthgren 1997). In order to sketch the basic principle of transforming the output into polar coordinates, we initially assume that exactly two outputs $\boldsymbol{y} \in \mathbb{R}^2_{\geq 0}$ are generated by a finite number of inputs. As illustrated in Fig. 1, any output combination (y_1, y_2) can be characterized by the norm of the vector $\boldsymbol{y}$ and the associated angle ϑ.

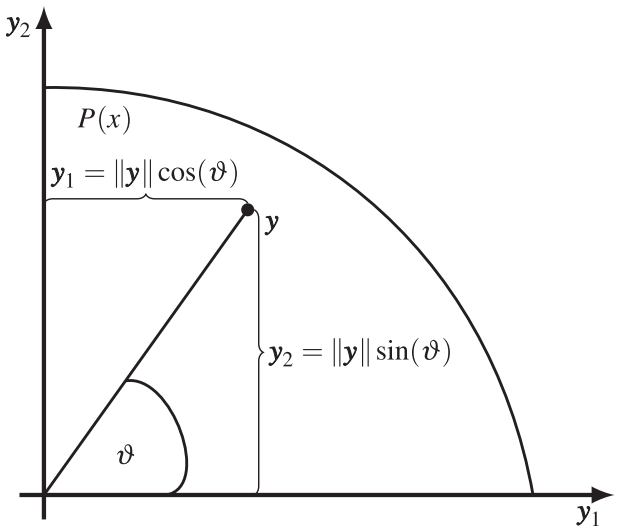

Fig. 1 Graphical representation of a two-dimensional output via polar coordinates

Thus, formally, the following applies in the simple two-output case:

$$\boldsymbol{y} = \begin{pmatrix} y_1 \\ y_2 \end{pmatrix} = l \cdot \begin{pmatrix} m_1(\vartheta) \\ m_2(\vartheta) \end{pmatrix}$$

whereby $l = l(\boldsymbol{y}) = \| \boldsymbol{y} \| = \sqrt{y_1^2 + y_2^2}$ is the Euclidean length of the vector $\boldsymbol{y}$, and

$$m_1(\vartheta) = \frac{y_1}{\| \boldsymbol{y} \|} = \cos(\vartheta), \tag{11}$$

$$m_2(\vartheta) = \frac{y_2}{\| \boldsymbol{y} \|} = \sin(\vartheta) \tag{12}$$

with

$$\vartheta = \vartheta(\boldsymbol{y}) \in \left[0, \frac{\pi}{2}\right] \tag{13}$$

indicates the transformation into polar coordinates. Eqs. (11) and (12) represent the trigonometric relationships between the angle ϑ and the norm of the vector $\boldsymbol{y}$, as shown in Fig. 1. The values of ϑ can vary between 0° and 90°, which in radians corresponds to the closed interval from 0 to $\frac{\pi}{2}$ (see (13)).

In the case of a general s-dimensional output $\boldsymbol{y} \in \mathbb{R}^s_{\geq 0}$, the following results hold for the polar coordinate representation:

$$\boldsymbol{y} = l \cdot m(\boldsymbol{\vartheta}) \tag{14}$$

with

$$l = l(\boldsymbol{y}) = \| \boldsymbol{y} \| = \sqrt{\sum_{r=1}^{s} y_r^2}, \tag{15}$$

$$m_r(\boldsymbol{\vartheta}) = \frac{y_r}{\| \boldsymbol{y} \|} = \cos(\vartheta_r) \prod_{i=0}^{r-1} \sin(\vartheta_i), \; r = 1, \ldots, s, \tag{16}$$

$$\boldsymbol{\vartheta} = \vartheta(\boldsymbol{y}) \in \left[0, \frac{\pi}{2}\right]^{s-1}, \; \sin(\vartheta_0) = \cos(\vartheta_s) = 1. \tag{17}$$

Thus, in the case of an s-dimensional output, there are $s-1$ angles $\vartheta_1, \ldots, \vartheta_{s-1}$, which can be calculated recursively by

$$\vartheta_r = \arccos\left(\frac{y_r}{\| \boldsymbol{y} \| \prod_{i=0}^{r-1} \sin(\vartheta_i)}\right), \; r = 1, \ldots, s. \tag{18}$$

After transforming the multi-dimensional output into polar coordinates (see (14)-(17)), a multiple-output ray production function $g(\boldsymbol{x},\vartheta(\boldsymbol{y}))$ can be defined, which maps the maximum of the output-norm for a given direction of the outputs (represented by angles $\boldsymbol{\vartheta}$) and the given inputs $\boldsymbol{x}$

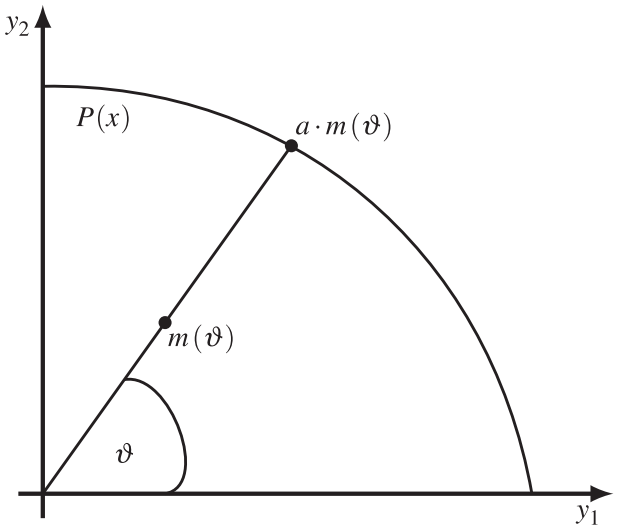

Fig. 2 Graphical representation of a ray production function in the case of a two-dimensional output

(Löthgren 1997):

$$g(\boldsymbol{x}, \vartheta(\boldsymbol{y})) = \max\{a \in \mathbb{R}_{\geq 0} | a \cdot m(\vartheta(\boldsymbol{y})) \in \boldsymbol{P}(\boldsymbol{x})\}. \tag{19}$$

Thus, the maximum length $a \in \mathbb{R}_{\geq 0}$ of the vector $m(\vartheta(\boldsymbol{y}))$ is determined by (19), such that $a \cdot m(\vartheta(\boldsymbol{y}))$ still belongs to the production possibility set. We again illustrate this idea in the case of a two-dimensional output in Fig. 2.

According to (14), $\boldsymbol{y} = l \cdot m(\boldsymbol{\vartheta})$ holds, and by definition (19) $g(\boldsymbol{x}, \vartheta(\boldsymbol{y})) \cdot m(\boldsymbol{\vartheta})$ belongs to the isoquant of the production possibility set Isoq$\boldsymbol{P}(\boldsymbol{x})$ (Löthgren 1997). Therefore, the output distance function, as defined in (3), can be demonstrated by

$$\begin{aligned} D_O(\boldsymbol{x}, \boldsymbol{y}) = \; & \frac{\|\boldsymbol{y} \cdot m(\boldsymbol{\vartheta})\|}{\|g(\boldsymbol{x}, \vartheta(\boldsymbol{y})) \cdot m(\boldsymbol{\vartheta})\|} = \frac{\|\boldsymbol{y}\|}{g(x, \vartheta(y))} \\ & \Leftrightarrow \| \boldsymbol{y} \| = g(\boldsymbol{x}, \vartheta(\boldsymbol{y})) \cdot e^{-u}. \end{aligned} \tag{20}$$

Analogously to (10), a noise term v has to be included to account for measurement and approximation errors:

$$\| \boldsymbol{y} \| = g(\boldsymbol{x}, \vartheta(\boldsymbol{y})) \cdot e^{v-u}. \tag{21}$$

These transformations result in a one-dimensional regression Eq. (21), in which the output norm is the dependent variable and the inputs as well as the angles associated with $\boldsymbol{y}$ are the regressors in the model. The transformation into polar coordinates does not impose any additional requirements on the set of potential functions for estimating the inefficiencies by StoNED. Therefore, a ray production function appears to be a fruitful and meaningful approach for modeling production systems with multi-dimensional input and output.

3 Ray production function and StoNED

Before we describe the approach for estimating the inefficiency of production systems with multi-dimensional input and output by StoNED, we must analyze the conditions that a ray production function has to fulfill in order for StoNED to be applicable. Firstly, we have to ensure that a ray production function is an analogous representation of the technology $\boldsymbol{T}$ and that convex output sets $P(\boldsymbol{x})$ will be generated. One necessary condition for this requirement to be fulfilled is the weak disposability of all outputs, because then, according to Löthgren (1997), the following applies:

$$\| \boldsymbol{y} \| \leq g(\boldsymbol{x}, \vartheta(\boldsymbol{y})) \Leftrightarrow \boldsymbol{y} \in P(\boldsymbol{x}).$$

If strong input disposability is additionally assumed, a ray production function is positively monotonic in its inputs (Löthgren 1997).

Furthermore, we must ensure that the angles $\boldsymbol{\vartheta}$ of the polar coordinate representation are not correlated with the error terms. In other words, there must be no endogeneity and, thus, no relationship between the explanatory variables $\boldsymbol{\vartheta}$ and the error terms. In analogy to Löthgren (2000), we consider an output $\boldsymbol{y} \in \mathbb{R}^s_{\geq 0}$ that can be represented by its polar coordinates:

$$\begin{aligned} \boldsymbol{y} &= \| \boldsymbol{y} \| \cdot m(\vartheta(\boldsymbol{y})) \\ &\Leftrightarrow m(\vartheta(\boldsymbol{y})) = \tfrac{\boldsymbol{y}}{\|\boldsymbol{y}\|} \\ &\Leftrightarrow \vartheta(\boldsymbol{y}) = m^{-1}\left(\tfrac{\boldsymbol{y}}{\|\boldsymbol{y}\|}\right). \end{aligned} \tag{22}$$

By means of equivalent transformations, a description of the angles results via the inverse of the function $m(\cdot)$ (see (16)). If ε is an error term, which according to the selected model leads to a disturbed output $\tilde{\boldsymbol{y}} = \boldsymbol{y} \cdot e^{\varepsilon}$, then the following holds:

$$\begin{aligned} \vartheta(\tilde{\boldsymbol{y}}) &= m^{-1}\left(\frac{\tilde{\boldsymbol{y}}}{\| \tilde{\boldsymbol{y}} \|}\right) = m^{-1}\left(\frac{\boldsymbol{y} \cdot e^{\varepsilon}}{\| \boldsymbol{y} \cdot e^{\varepsilon} \|}\right) \\ &= m^{-1}\left(\frac{\boldsymbol{y}}{\| \boldsymbol{y} \|}\right) = \vartheta(\boldsymbol{y}). \end{aligned}$$

Even though disturbances such as ε are considered, the angles of the polar coordinate representation of $\tilde{\boldsymbol{y}}$ and $\boldsymbol{y}$ are identical. Thus, in the above-mentioned model, there is no correlation between the angles $\boldsymbol{\vartheta}$ and the error term ε.

After clarification of the necessary assumptions and properties, and starting from the regression Eq. (21), linearization yields the initial equation to be estimated by StoNED. With $\varepsilon = v - u$, the following applies:

$$\begin{aligned} &\| \boldsymbol{y} \| = g(\boldsymbol{x}, \vartheta(\boldsymbol{y})) \cdot e^{\varepsilon} \\ \Leftrightarrow\ &\ln \| \boldsymbol{y} \| = \ln(g(\boldsymbol{x}, \vartheta(\boldsymbol{y}))) + \varepsilon. \end{aligned} \tag{23}$$

By means of a CNLS regression, the form of the function to be estimated can now be determined by StoNED, where $\ln(\| \boldsymbol{y} \|)$ is the dependent variable and $\boldsymbol{z} = (x_1, \ldots, x_m, \vartheta_1, \ldots, \vartheta_{s-1})^t$ are the independent variables. For this purpose, the subsequent quadratic optimization problem with n DMUs ($j = 1, \ldots, n$) has to be solved (by analogy to Kuosmanen and Kortelainen 2012):

$$\begin{aligned} \min_{\varepsilon_{CNLS}, \alpha, \beta} \ & \sum_{j=1}^{n} \varepsilon_{j,CNLS}^2 \\ & \ln(\| \boldsymbol{y}_j \|) = \ln\left(\alpha_j + \boldsymbol{\beta}_j^t \boldsymbol{z}_j\right) + \varepsilon_{j,CNLS} \ \forall j = 1, \ldots, n \\ & \alpha_j + \boldsymbol{\beta}_j^t z_j \leq \alpha_h + \boldsymbol{\beta}_h^t z_j \ \forall j, h = 1, \ldots, n \\ & \boldsymbol{\beta}_j \geq \boldsymbol{0} \ \forall j = 1, \ldots, n. \end{aligned} \tag{24}$$

Unlike the residuals of ordinary least squares (OLS) regression used in SFA, the problem can arise with CNLS regression that the residuals $\varepsilon_{j,CNLS}$ are correlated with the explanatory variables. This situation can occur, since the monotonicity and concavity constraints of the CNLS regression may affect the sample correlation of the residuals and explanatory variables. Correlation between the residual and explanatory variables can in turn lead to problems in practical applications, for example when deciding how the outputs should be ordered and hence which angles should be considered. We analyze this problem in more detail in Section 4 by conducting Monte Carlo simulations.

As Seijo and Sen (2011) as well as Lim and Glynn (2012) have proven, the CNLS estimators $\hat{\varepsilon}_{j,CNLS}$ are consistent when using models with only noise. Andor and Hesse (2014) stated, that these estimators are biased by $E[u_j]$ when using models with noise and inefficiency. Based on the CNLS residuals $\hat{\varepsilon}_{j,CNLS}$, the expected inefficiency and thus the unbiased residuals $\hat{\varepsilon}_j$ can be estimated using, e.g., the method of moments or pseudolikelihood estimation. Thereby, additional distribution assumptions for the inefficiency term and the noise term have to be made. However, Kuosmanen et al. (2015a) as well as Kuosmanen and Johnson (2017) show that no distribution assumptions are necessary when using kernel deconvolution (Hall and Simar 2002).[3] Since we demonstrate the method of moments in the following, we assume that the inefficiency u_j follows a half-normal distribution with positive expected value μ and finite variance σ_u^2, and that the noise term v_j follows a normal distribution with expected value 0 and finite variance σ_v^2. The random variables are stochastically

[3] But other assumptions are necessary. For example, discontinuity at zero for the ineffciency distribution is needed and the variance of the noise term has to converge to zero if the sample size goes to infinity.

independent and identically distributed (i.i.d.): [4]

$$\begin{matrix} u_j \overset{i.i.d.}{\sim} \left|\mathcal{N}\left(0,\sigma_u^2\right)\right| \\ v_j \overset{i.i.d.}{\sim} \mathcal{N}\left(0,\sigma_v^2\right) \end{matrix} \quad \forall j = 1, \ldots, n. \tag{25}$$

The second and third moments are initially determined from the CNLS residuals $\hat{\varepsilon}_{j,CNLS}$ (Kuosmanen and Kortelainen 2012):

$$\hat{M}_2 = \sum_{j=1}^{n} \frac{\left(\hat{\varepsilon}_{j,CNLS} - \hat{E}[\varepsilon_{j,CNLS}]\right)^2}{n},$$

$$\hat{M}_3 = \sum_{j=1}^{n} \frac{\left(\hat{\varepsilon}_{j,CNLS} - \hat{E}[\varepsilon_{j,CNLS}]\right)^3}{n}.$$

$\hat{M}_2$ and $\hat{M}_3$ can now be used to assess the standard deviation of the inefficiency and noise term:

$$\hat{\sigma}_u = \sqrt[3]{\frac{\hat{M}_3}{\sqrt{\frac{2}{\pi}}\left(1-\frac{4}{\pi}\right)}},$$

$$\hat{\sigma}_v = \sqrt{\hat{M}_2 - \left(1-\frac{2}{\pi}\right)\cdot\hat{\sigma}_u^2}.$$

The expected inefficiency is calculated by $\hat{E}[u_j] = \sqrt{\frac{2}{\pi}}\cdot\hat{\sigma}_u$, resulting in consistent estimates of the residuals $\hat{\varepsilon}_j$:

$$\hat{\varepsilon}_j = \hat{\varepsilon}_{j,CNLS} - \sqrt{\frac{2}{\pi}}\cdot\hat{\sigma}_u.$$

A consistent and unbiased estimator for the function value is determined similarly:

$$\hat{f}^{StoNED}(\boldsymbol{z}_j) = \hat{\alpha}_j + \hat{\boldsymbol{\beta}}_j^t \boldsymbol{z}_j + \sqrt{\frac{2}{\pi}}\cdot\hat{\sigma}_u.$$

The efficiency of each DMU $j = 1, \ldots, n$, can now be determined with the point estimator, either according to Battese and Coelli (1988), or according to Jondrow et al. (1982). The disadvantage of both point estimators is that they are not consistent estimators for the u_j for cross-sectional data. However, Battese and Coelli's point estimator is at least consistent for an infinite time horizon. Additionally it is optimal in the sense of minimizing the standard deviation (Andor and Hesse 2014), as well as being mainly used in empirical and theoretical applications (Bogetoft and Otto 2011). This is why we use it in our Monte Carlo simulation in Section 4. It is defined as follows:

$$\hat{E}\left[e^{-u_j}|\hat{\varepsilon}_j\right] = \frac{1-\Phi\left(\hat{\sigma}_* - \frac{\hat{\mu}_{j*}}{\hat{\sigma}_*}\right)}{1-\Phi\left(-\frac{\hat{\mu}_{j*}}{\hat{\sigma}_*}\right)}\cdot e^{-\hat{\mu}_{j*}+\frac{1}{2}\hat{\sigma}_*^2}$$

with $\hat{\sigma}_* = \frac{\hat{\sigma}_u\hat{\sigma}_v}{\sqrt{\hat{\sigma}_u^2+\hat{\sigma}_v^2}}$, and $\hat{\mu}_{j*} = -\frac{\hat{\varepsilon}_j\hat{\sigma}_u^2}{\sqrt{\hat{\sigma}_u^2+\hat{\sigma}_v^2}}$.

4 Monte Carlo simulation

There are numerous Monte Carlo simulations that analyze the quality of efficiency measurement methods. Besides simulations for production systems with multiple inputs and exactly one output (e.g. Badunenko et al. 2012; Gong and Sickles 1992; Olson et al. 1980; Ruggiero 1999), simulations for production systems with multiple inputs and multiple outputs exist as well. For instance, Resti (2000) compares the quality of stochastic frontiers, DEA, and stochastic DEA by simulating data with two inputs and three outputs. Perelman and Santín (2009) show how a production with two inputs and outputs can be displayed via an output distance function, and analyze the quality of efficiency measurements using DEA subject to sample size and output ratios. On this basis, Henningsen et al. (2015) analyze the quality of efficiency measurements by SFA when the technology of the underlying production system with two inputs and outputs is modeled via an output distance function or a ray production function.

In the following, we also use a Monte Carlo simulation to evaluate the quality of the frontier and efficiencies estimated by StoNED when modeling multiple outputs with a ray production function. We refer to the above mentioned literature by adopting elements of the simulation designs. Below, we introduce our Monte Carlo simulation, presenting its results after discussing its design.

4.1 Data generating process and design[5]

For the simulation, we consider a production system that transforms two inputs $\boldsymbol{x} \in \mathbb{R}^2_{\geq 0}$ into two outputs $\boldsymbol{y} \in \mathbb{R}^2_{\geq 0}$. In order to investigate the influence of different production technologies, we regard three different technologies. As in Perelman and Santín (2009), as well as in Henningsen et al. (2015), we first consider a translog function defined as follows:

$$\ln(\|\boldsymbol{y}\|) = \alpha_0 + \alpha_1\vartheta + 0.5\alpha_{11}\vartheta^2 + \sum_{j=1}^{2}\beta_j\ln(x_j) + 0.5\sum_{i=1}^{2}\sum_{l=1}^{2}\beta_{il}\ln(x_i)\ln(x_l) + \sum_{i=1}^{2}\gamma_{1i}\vartheta\ln(x_i). \tag{26}$$

The choice of the parameters α_0,α_1,α_{11},β_j,β_{il} and γ_{1i} with $j, i, l = 1, 2$ allows the functional form and the returns to scale properties to be specified. Below, we adjust these

[4] The distributional assumptions could be modified, for example, by implying an exponential distribution for the inefficiency term (see Kumbhakar and Lovell 2003).

[5] We used GAMS for the implementation of the simulation design. The code is available upon request from us.

parameters to define both constant returns to scale (TL CRS) and decreasing returns to scale (TL DRS). In order to investigate the effect of choosing a different functional form, we also consider a logarithmized quadratic function (Q) with the following expression:

$$\ln(\| \boldsymbol{y} \|) = \ln\left(\begin{array}{c}\alpha_0 + \beta_1 x_1 + \beta_2 x_2 + \alpha_1 \vartheta + \beta_{11}(x_1+\gamma_1)^2 + \\ \beta_{22}(x_2+\gamma_2)^2 + \alpha_{11}(\vartheta+\gamma_3)^2\end{array}\right). \tag{27}$$

To ensure that the three technologies are comparable, the input amounts are simulated as uniformly distributed random variables in the interval [5;15]. The parameters of each technology were also adjusted correspondingly so that the resulting output is contained in the interval [1;4.5].[6] Returning to the approach described in Perelman and Santín (2009), the ratio of the logarithmized outputs is generated as a uniformly distributed random variable in the interval $|\ln(y_2) - \ln(y_1)| \leq 1.5$. According to (18), the angle ϑ corresponding to this output ratio can be determined as follows:

$$\vartheta = \arccos\left(\frac{1}{\sqrt{1+e^{2(\ln(y_2)-\ln(y_1))}}}\right). \tag{28}$$

Given the simulated input quantities, the resulting angle, and the selected parameters, the fully efficient output quantities can be calculated according to (26) and (27). Finally, these output quantities are disturbed by inefficiency and noise, which are modeled as half-normally distributed and normally distributed random variables, respectively. Thus, the observed output quantities can be calculated from (21).

As well as varying the functional form and the returns to scale properties, we make further specifications. We distinguish between the number of considered DMUs by setting $n = 25$, 50, 100, 200, and 400. For the standard deviation of the inefficiency term, we choose $\sigma_u = 0.15$. Thus, true efficiencies with an average of 88% are generated for the considered DMUs. We modify the occurring noise according to different noise-to-signal ratios $\rho_{nts} = \frac{\sigma_v}{\sigma_u}$ with $\rho_{nts} = 0$, 0.5, 1, and 2.

Overall, there are 60 scenarios, for each of which $M = 500$ replications are generated, giving a total of 30,000 replications. For these replications, the frontiers and efficiencies are determined both by StoNED and, for comparison, by SFA and by DEA. For SFA, we distinguish between inefficiency estimates based on an assumed Cobb-Douglas function (SFA CD) and a translog function (SFA TL) (Aigner et al. 1977; Meeusen and van den Broeck 1977). For DEA, we differentiate between the basic models (CCR and BCC), i.e. between radial models with constant (DEA CCR) and variable (DEA BCC) returns to scale (Charnes et al. 1978; Banker et al. 1984). The estimation of inefficiencies, both by StoNED and in the two SFA variants, is based on the method of moments. As described in Section 3, we assume a half-normal distribution for the inefficiency term and a normal distribution for the noise term (see (25)). According to Olson et al. (1980) and Banker et al. (1993), estimation problems can occur if the following requirements are not met: On the one hand, the estimate of the third moment must be negative; on the other hand, the estimated standard deviation of the noise component must be positive. If these conditions are not fulfilled, we follow the suggestion by Kuosmanen and Kortelainen (2012) and set the value of the third moment to -0.0001 (which is equivalent to setting the variance of the inefficiency term to this value) and/or the value of the standard deviation to 0.0001.

To validate the estimated frontier and efficiencies calculated by StoNED, SFA CD, SFA TL, DEA CCR, or DEA BCC, we use three standard assessment criteria. First, the mean absolute deviation (MAD) between the true frontier f and the frontier estimates $\hat{f}$, as well as between the true efficiencies θ and the estimated efficiencies $\hat{\theta}$ is calculated:

$$\mathrm{MAD}_f = \frac{1}{nM}\sum_{k=1}^{M}\sum_{j=1}^{n}|\hat{f}_k(\boldsymbol{z}_j) - f_k(\boldsymbol{z}_j)|, \tag{29}$$

$$\mathrm{MAD}_\theta = \frac{1}{nM}\sum_{k=1}^{M}\sum_{j=1}^{n}|\hat{\theta}_{k,j} - \theta_{k,j}|. \tag{30}$$

In addition the mean deviation (MD) is determined. This criteria allows an identification of both potential overestimation and underestimation of these estimates:

$$\mathrm{MD}_f = \frac{1}{nM}\sum_{k=1}^{M}\sum_{j=1}^{n}\left(\hat{f}_k(\boldsymbol{z}_j) - f_k(\boldsymbol{z}_j)\right), \tag{31}$$

$$\mathrm{MD}_\theta = \frac{1}{nM}\sum_{k=1}^{M}\sum_{j=1}^{n}\left(\hat{\theta}_{k,j} - \theta_{k,j}\right). \tag{32}$$

Finally, the mean squared error (MSE) is calculated, from which the variance of the deviations can be determined:

$$\mathrm{MSE}_f = \frac{1}{nM}\sum_{k=1}^{M}\sum_{j=1}^{n}(\hat{f}_k(\boldsymbol{z}_j) - f_k(\boldsymbol{z}_j))^2, \tag{33}$$

$$\mathrm{MSE}_\theta = \frac{1}{nM}\sum_{k=1}^{M}\sum_{j=1}^{n}(\hat{\theta}_{k,j} - \theta_{k,j})^2. \tag{34}$$

[6] The three technologies used here are consistent with the convexity and free disposability axioms. To check this, we first performed a pre-simulation to generate data without inefficiency and noise. These data were used to show that StoNED and DEA BCC estimate both the frontier and efficiencies exactly and thus that each technology satisfies the required properties.

Table 1 Overview of the mean absolute deviation results in regard to the frontier

	All scenarios		Scenarios without noise		Scenarios with noise	
	MAD	Rank (MAD)	MAD	Rank (MAD)	MAD	Rank (MAD)
StoNED	0.0650	2.03	0.0350	2.20	0.0791	2.56
SFA CD	0.0636	2.07	0.0424	2.87	0.0707	1.80
SFA TL	0.0630	1.82	0.0338	1.67	0.0728	1.87
DEA CCR	0.2239	4.58	0.1050	4.20	0.2635	4.71
DEA BCC	0.1506	4.07	0.0562	4.07	0.1836	4.07

MAD Mean absolute deviation

Table 2 Overview of the mean absolute deviation results in regard to the efficiency

	All scenarios		Scenarios without noise		Scenarios with noise	
	MAD	Rank (MAD)	MAD	Rank (MAD)	MAD	Rank (MAD)
StoNED	0.0598	2.28	0.0310	2.20	0.0694	2.31
SFA CD	0.0585	2.42	0.0343	2.73	0.0666	2.31
SFA TL	0.0563	1.45	0.0305	1.67	0.0648	1.38
DEA CCR	0.1675	4.78	0.0859	4.27	0.1946	4.96
DEA BCC	0.1212	4.07	0.0508	4.13	0.1446	4.04

MAD Mean absolute deviation

4.2 Overview

Due to limited additional information when comparing all three assessment criteria, we only provide an overview of the results in terms of the MAD criterion and the five considered methods for the deviations of the frontier and efficiencies. [7] The results of the two remaining assessment criteria are presented in the appendix (Table 9–11). We differentiate between the averages taken over all scenarios (= 60 scenarios) and, additionally, the averages taken over all scenarios without noise (= 15 scenarios) as well as with noise (= 45 scenarios) for the deviations of the frontier in Table 1. In addition, the average rank of each method is given.

The MAD values of the stochastic methods are small, although these values increase as the noise increases.[8] In contrast, the deviations of both DEA variants are higher. Although the deviations are comparable to the stochastic methods in the scenarios without noise, the DEA variants perform remarkably worse in the presence of noise. The results of the CCR model are weaker than those of the BCC model.[9] When comparing all methods in terms of the quality of their estimates, the stochastic models appear to outperform DEA. Concerning the three stochastic methods, the values of SFA TL, StoNED and SFA CD lie within in a very close margin.

Table 2 gives another overview of the MAD results of all five methods, this time focusing on the difference between the true efficiencies and the efficiencies estimated by each method. The table again considers all 60 scenarios, as well as scenarios without and with noise.

The same tendencies observed in the deviations of the frontier may again be detected in the efficiency estimates. We see again that the stochastic methods outperform the DEA models; even when the data do not include noise. Overall, StoNED and SFA result in MADs of 0.0563 to 0.0598. These average deviations are as high as 0.1212 (BCC) or even 0.1675 (CCR) in the DEA models. Although these high deviations may of course be ascribed to the scenarios with noise, the MADs are relatively high even in the scenarios without noise. If we compare the stochastic methods among themselves, SFA TL proves to be slightly superior here. [10] However, StoNED achieves a similar performance.

All results are quite plausible. For instance, Andor and Hesse (2014) previously reported that the stochastic methods SFA and StoNED lead to lower average absolute deviations than the DEA models. Our observation that SFA TL is slightly superior was also reported by Andor and Hesse (2014) in the case of a one-dimensional output. In summary, we determine that estimating the frontier and efficiencies with StoNED seems to lead to plausible and meaningful results when a ray production function is used to represent a multi-dimensional output.

4.3 Consideration of individual effects

We now consider the individual effects of modifying the number of DMUs (Table 3), the noise-to-signal ratio (Table 4) and the functional form on the estimation of the frontier (Table 5). For conciseness, we again focus exclusively on

[7] Since the stochastic methods StoNED and SFA minimize the sum of squared errors, these methods should perform better on the MSE criteria than on the MAD criteria. If we regard the following analyses concerning the MSE criteria the measures are indeed better than the MAD measures. However, the following general statements are also valid when regarding MSE measures. Therefore, we abstain from presenting the MSE results in detail.

[8] When additionally taking the MD into account, the deviations are almost zero. This shows that under- and overestimations of the true frontier mutually balance each other out. StoNED and SFA CD tend to slightly underestimate the frontier in scenarios without noise, and slightly overestimate them in scenarios with noise. Also the MSE values are small, which suggests that the stochastic methods tend to generate many small deviations but no large ones.

[9] Additionally, the MSE shows that DEA tend to generate high deviations of single DMUs (see Table 11), which is plausible considering the deterministic nature of DEA.

[10] In 43 of 60 scenarios SFA TL is ranked on the first place.

Table 3 Variation of sample size

		Scenarios without noise			Scenarios with noise		
	Number of DMUs	TL CRS	TL DRS	Q	TL CRS	TL DRS	Q
StoNED	25	0.0604	0.0541	0.0521	0.1171	0.1105	0.1020
	50	0.0464	0.0410	0.0398	0.1000	0.0925	0.0881
	100	0.0347	0.0317	0.0298	0.0826	0.0792	0.0697
	200	0.0272	0.0258	0.0227	0.0683	0.0650	0.0576
	400	0.0219	0.0207	0.0167	0.0552	0.0519	0.0467
SFA CD	25	0.0563	0.0564	0.0444	0.0946	0.0946	0.0865
	50	0.0525	0.0519	0.0326	0.0828	0.0811	0.0731
	100	0.0484	0.0483	0.0241	0.0717	0.0735	0.0588
	200	0.0464	0.0468	0.0199	0.0658	0.0666	0.0499
	400	0.0457	0.0457	0.0172	0.0602	0.0598	0.0412
SFA TL	25	0.0616	0.0623	0.0625	0.1113	0.1117	0.1113
	50	0.0437	0.0426	0.0425	0.0871	0.0862	0.0878
	100	0.0288	0.0293	0.0281	0.0674	0.0684	0.0665
	200	0.0205	0.0212	0.0193	0.0549	0.0551	0.0540
	400	0.0156	0.0155	0.0132	0.0441	0.0437	0.0424
DEA CCR	25	0.0647	0.1141	0.0994	0.1353	0.1960	0.1797
	50	0.0476	0.1335	0.1083	0.1624	0.2451	0.2233
	100	0.0341	0.1545	0.1222	0.2082	0.2998	0.2735
	200	0.0237	0.1750	0.1367	0.2543	0.3577	0.3255
	400	0.0167	0.1940	0.1501	0.3009	0.4130	0.3777
DEA BCC	25	0.0886	0.0826	0.0859	0.1345	0.1369	0.1343
	50	0.0717	0.0646	0.0721	0.1406	0.1516	0.1464
	100	0.0551	0.0494	0.0585	0.1671	0.1827	0.1718
	200	0.0412	0.0367	0.0454	0.2026	0.2209	0.2070
	400	0.0303	0.0266	0.0345	0.2448	0.2648	0.2481

Performance criterion: mean absolute deviation between the true production function and the estimated frontier

TL CRS Translog function with constant returns to scale, *TL DRS* Translog function with decreasing returns to scale, *Q* Logarithmized quadratic function

the MAD criterion. Since there are no differences in the results between estimations of frontiers and efficiencies, we additionally focus exclusively on the frontier estimation in the following.[11]

The MADs clearly show that the accuracy of the frontier estimates of StoNED and the SFA variants improves as the number of considered DMUs increases. In regard to DEA this statement is not generally valid. For scenarios with noise, the MADs increase for both DEA CCR and DEA BCC; in contrast, for scenarios without noise, the MADs increase only for DEA CCR (with the exception of a translog function with constant returns to scale). These effects are essentially as expected (see e.g. Banker et al. 1993; Coelli 1995), and has already been shown in other simulations (see e.g. Andor and Hesse 2014; Henningsen et al. 2015). The quality of the individual methods relative to each other does not change in practice when the number of DMUs is varied.

In Table 4, the MAD results are classified with regard to the noise-to-signal ratio. For simplification reasons, we clustered the scenarios in regard to the number of DMUs. The column "Low number of DMUs" subsumes scenarios with 25 and 50 DMUs; accordingly the column "High number of DMUs" subsumes scenarios with 100, 200, and 400 DMUs.

The mean absolute deviation increases as the noise increases, which is an expected and plausible effect, since several studies have shown this (e.g., see Badunenko et al. 2012; Jensen 2005; Ondrich and Ruggiero 2001). We note that the quality of the StoNED estimates decreases much more sharply than the two SFA variants at the high noise-to-signal ratio of $\rho_{nts} = 2$. It is however worth questioning whether efficiency measurement is meaningful with such noisy data (see Andor and Hesse 2014). Interestingly, at higher noise-to-signal ratios, the frontier generated by the

[11] The MAD results of the efficiency estimation are shown in Tables 12 and 13 in the appendix.

Table 4 Variation of noise-to-signal-ratio

		TL CRS		TL DRS		Q	
	Number of DMUs	Low	High	Low	High	Low	High
	ρ_{nts}						
StoNED	0	0.0534	0.0280	0.0476	0.0261	0.0459	0.0231
	0.5	0.0618	0.0357	0.0576	0.0337	0.0526	0.0289
	1	0.0898	0.0561	0.0835	0.0531	0.0760	0.0467
	2	0.1741	0.1144	0.1634	0.1092	0.1566	0.0984
SFA CD	0	0.0544	0.0468	0.0542	0.0469	0.0385	0.0204
	0.5	0.0593	0.0501	0.0604	0.0502	0.0475	0.0270
	1	0.0757	0.0586	0.0752	0.0588	0.0672	0.0426
	2	0.1311	0.0889	0.1281	0.0908	0.1247	0.0804
SFA TL	0	0.0526	0.0216	0.0524	0.0220	0.0525	0.0202
	0.5	0.0603	0.0292	0.0624	0.0293	0.0613	0.0284
	1	0.0842	0.0482	0.0846	0.0474	0.0843	0.0466
	2	0.1530	0.0891	0.1500	0.0906	0.1531	0.0879
DEA CCR	0	0.0562	0.0249	0.1238	0.1745	0.1038	0.1364
	0.5	0.0533	0.0694	0.1379	0.2080	0.1188	0.1710
	1	0.1024	0.1949	0.1820	0.2956	0.1592	0.2650
	2	0.2909	0.4990	0.3417	0.5668	0.3266	0.5407
DEA BCC	0	0.0802	0.0422	0.0736	0.0376	0.0790	0.0461
	0.5	0.0755	0.0577	0.0681	0.0603	0.0712	0.0518
	1	0.1000	0.1502	0.1035	0.1666	0.0967	0.1527
	2	0.2371	0.4065	0.2611	0.4414	0.2531	0.4223

Performance criterion: mean absolute deviation between the true production function and the estimated frontier. Low numbers of DMUs: Scenarios with 25 and 50 DMUs, High numbers of DMUs: Scenarios with 100, 200, and 400 DMUs

TL CRS Translog function with constant returns to scale, *TL DRS* Translog function with decreasing returns to scale, *Q* Logarithmized quadratic function, ρ_{nts} noise-to-signal ratio

DEA models performs increasingly poorly as the number of considered DMUs increases.

The effects of modifying the form of the underlying technology are shown in Table 5. Again, we clustered the scenarios concerning the number of DMUs. We see that only for DEA CCR there are high differences between the estimations. As expected, DEA CCR estimates the translog function with constant returns to scale and its efficiencies distinctly better than it does concerning the translog function with decreasing returns to scale and the quadratic function. Both StoNED and SFA CD, however, tend to produce a slightly better estimate for the quadratic function, whereas SFA TL performs slightly better on both variants of the translog function.

4.4 Correlation between residuals and angles

As noted in Section 3, by using CNLS regression we cannot necessarily guarantee that the residuals and the angles are uncorrelated. Furthermore, the effect of changing the order of the outputs on the estimation is unclear. To shed some light on this discussion, we analyze the consequences for the main simulation and additional simulations in the following.

We calculate the correlation between the chosen angle ϑ and the estimated residuals of the stochastic methods in each of the 60 scenarios considered by our simulation. In regard to SFA, we found that the residuals and angles are uncorrelated in every scenario. Since SFA uses OLS regression, where the correlation is zero by construction (Wooldridge 2013), these findings are plausible.

However, we cannot necessarily expect the same to hold for CNLS regression, as used by StoNED. The Pearson (1896) correlation coefficients of the StoNED estimates are therefore listed in Table 6. Since no correlation was observed between the value of the correlation coefficients and the number of considered DMUs, Table 6 does not distinguish between the number of DMUs, for conciseness. We can see that the choice of underlying production technology affects the correlation between the residuals and the angles, since there is no correlation for either of the two translog technologies, but the residuals and the angles of the quadratic function are slightly correlated. This correlation increases weakly as the noise-to-signal ratio becomes larger.

Table 5 Variation of functional form

		Scenarios without noise		Scenarios with noise	
	Number of DMUs	Low	High	Low	High
StoNED	TL CRS	0.0534	0.0280	0.1085	0.0687
	TL DRS	0.0476	0.0261	0.1015	0.0654
	Q	0.0459	0.0231	0.0951	0.0580
SFA CD	TL CRS	0.0544	0.0468	0.0887	0.0659
	TL DRS	0.0542	0.0468	0.0887	0.0666
	Q	0.0385	0.0204	0.0798	0.0500
SFA TL	TL CRS	0.0526	0.0216	0.0992	0.0555
	TL DRS	0.0524	0.0220	0.0990	0.0557
	Q	0.0525	0.0202	0.0996	0.0543
DEA CCR	TL CRS	0.0562	0.0249	0.1489	0.2544
	TL DRS	0.1238	0.1745	0.2206	0.3568
	Q	0.1038	0.1364	0.2015	0.3256
DEA BCC	TL CRS	0.0802	0.0422	0.1375	0.2048
	TL DRS	0.0736	0.0376	0.1442	0.2228
	Q	0.0790	0.0461	0.1403	0.2089

Performance criterion: mean absolute deviation between the true production function and the estimated frontier, Low numbers of DMUs: Scenarios with 25 and 50 DMUs; High numbers of DMUs: Scenarios with 100, 200, and 400 DMUs

TL CRS Translog function with constant returns to scale, *TL DRS* Translog function with decreasing returns to scale, *Q* Logarithmized quadratic function

Table 6 Pearson correlation coefficients between the residuals and the angles ϑ in all 60 scenarios

	TL CRS	TL DRS	Q
$\rho_{nts} = 0$	0	0	−0.06
$\rho_{nts} = 0.5$	0	0	−0.07
$\rho_{nts} = 1$	−0.01	−0.01	−0.08
$\rho_{nts} = 2$	−0.02	−0.01	−0.09

TL CRS Translog function with constant returns to scale, *TL DRS* Translog function with decreasing returns to scale, *Q* Logarithmized quadratic function, ρ_{nts} noise-to-signal ratio

Table 7 Pearson correlation coefficients between the residuals and the angles ϑ as well as opposite angles $\tilde{\vartheta}$

	CRS		DRS	
	ϑ	$\tilde{\vartheta}$	ϑ	$\tilde{\vartheta}$
$\rho_{nts} = 0$	−0.007	−0.005	−0.003	−0.013
$\rho_{nts} = 1$	−0.009	−0.007	−0.005	−0.020

CRS Function with constant returns to scale, *DRS* Function with decreasing returns to scale, ρ_{nts} noise-to-signal ratio

Since the angle is not logarithmized in our translog functions, which we choose based on Henningsen et al. (2015), we further examine whether the logarithmization of the angle as performed by Löthgren (1997, 2000) influences the correlation between the residuals and the angles. For this purpose, we conduct an additional simulation and modify the translog function as follows:

$$\ln(\| \boldsymbol{y} \|) = \alpha_0 + \alpha_1 \ln(\vartheta) + 0.5\alpha_{11} \ln(\vartheta)^2 + \sum_{j=1}^{2} \beta_j \ln(x_j) + 0.5 \sum_{i=1}^{2} \sum_{l=1}^{2} \beta_{il} \ln(x_i) \ln(x_l) + \sum_{i=1}^{2} \gamma_{1i} \ln(\vartheta) \ln(x_i). \tag{35}$$

We simulate eight scenarios, varying the number of DMUs ($n = 50$ and 200) and the noise-to-signal ratio ($\rho_{nts} = 0$ and 1). All other assumptions from Section 4.1 still hold. The average correlation coefficients are slightly higher in this simulation. However, they are still close to zero (between −0.01 and −0.03), allowing us to state that the residuals and the angles of translog functions remain uncorrelated. Thus, there is no evidence that logarithmization has any influence on the correlation between residuals and angles.

Finally, we examine the extent to which changing the order of the outputs affects the estimated frontier and efficiencies. Therefore, we perform another simulation of the eight scenarios listed above. In a real world application, the user is confronted with the problem that the size of the involved angle depends on the order of the outputs. To reproduce this scenario in the simulation design, it is necessary to change the data generating process from Section 4.1. Consequently, we directly determine output quantities from the quantities of two randomly generated inputs on the basis of functions with constant returns to scale (CRS) and decreasing returns to scale (DRS). Thereby, the length of the output vector can be determined as well as the angle ϑ according to (18) and the opposite angle $\tilde{\vartheta} = \frac{\pi}{2} - \vartheta$. The opposite angle is obtained in the two-dimensional case by switching the order of the outputs. We execute the CNLS regression (24) with the generated inputs and outputs both with the angle ϑ and with the opposite angle $\tilde{\vartheta}$ as regressor variable.

If we regard the correlation between the residuals and angles (Table 7), we can again state that there is no or only a very small correlation between these two parameters when the angle ϑ is considered. Additionally, there is also no or only a very small correlation when observing the opposite angle $\tilde{\vartheta}$.

To determine the correlation between the frontiers and the efficiencies, which are estimated using the angle ϑ and the opposite angle $\tilde{\vartheta}$, the corresponding average Pearson correlation coefficients and average Spearman's (1904) rank correlation coefficients are listed in Table 8. In nearly all of the cases, there are highly significant correlations between the datasets.

It becomes obvious that the correlations between the estimated frontiers are slightly higher than between the estimated efficiencies. However, both the rank correlations and the Pearson correlation coefficients are extremely high, which indicates that there is no effect of the order of the

Table 8 Correlation coefficients between the estimators using the angle and the opposite angle

	Number of DMUs	ρ_{nts}	Frontier		Efficiency	
			Pearson	Spearman	Pearson	Spearman
CRS	50	0	0.998	0.997	0.984	0.978
		1	0.994	0.994	0.984	0.982
	200	0	0.999	0.999	0.994	0.993
		1	0.996	0.998	0.992	0.993
DRS	50	0	0.996	0.995	0.980	0.975
		1	0.988	0.986	0.984	0.980
	200	0	0.998	0.998	0.991	0.990
		1	0.993	0.996	0.992	0.992

CRS Function with constant returns to scale, *DRS* Function with decreasing returns to scale, ρ_{nts} noise-to-signal ratio

outputs on the estimated frontier and efficiencies. Our simulation illustrates the robustness of the CNLS regression results and the robustness of the estimated frontier and efficiencies via StoNED concerning the order of outputs. This is consistent with Henningsen et al. (2017), who analyze the properties of a ray production function in more detail and show that a ray production function is invariant to the change of the order of the outputs when observing two outputs without a logarithmized angle.

5 Summary, limitations, and outlook

The majority of papers involving StoNED deals with production systems where several inputs are used to generate exactly one output. Kuosmanen et al. (2015a) as well as Kuosmanen and Johnson (2017) are the first who enhance StoNED to multi-dimensional output cases by using distance functions. In this paper, we analyze the extent to which a ray production function can be applied in order to model technologies with multi-dimensional input and output for StoNED.

First, we showed that a ray production function can completely represent the underlying technology and leads to convex output sets. Since no further modifications are necessary in order for StoNED to be applied, the properties previously identified in the literature with respect to CNLS regressions hold, such as the consistency of the estimator.

To evaluate the frontier and efficiencies estimations of StoNED, when modeling the technology using a ray production function, we performed a Monte Carlo simulation. To facilitate the interpretation, we compared these estimated results with the results of SFA and DEA. It was shown that StoNED leads to plausible results. Even when the number of DMUs and the noise-to-signal ratio were varied, as well as the returns to scale properties and the form of the function, the values of the considered assessment criteria matched those of other known simulations. The SFA TL in particular tends to lead to the lowest mean absolute deviations, although the MAD values of StoNED are only slightly higher. One major problem with CNLS regression is that the residuals can correlate with the explanatory variables. With our Monte Carlo simulation, we showed that there is no such correlation with the translog functions, and there are only low levels of correlation with the logarithmized quadratic function. We also demonstrated that changing the order of two considered outputs did not lead to different frontier or efficiency estimates.

However, the use of a ray production function is subject to some limitations (see Henningsen et al. 2017), of which we discuss the two most important ones in the following and which indicate the need for further research in regard to the application with StoNED. Firstly, a ray production function is not scale-invariant, meaning that it is not irrelevant for a user as to which scale the quantities of inputs and outputs are measured on. Since we have modeled all inputs and outputs in the same order of magnitude, this property of a ray production function has no effect in regard to our simulation results. But this would hardly be the case in real world scenarios. It should therefore be analyzed how the function and efficiency estimations react when the scales of inputs and outputs are changed.

The second important limitation concerns the order of the outputs which are included in the efficiency analysis. As already mentioned, Henningsen et al. (2017) state that the order of the outputs has no influence on the modeling when a ray production function is used for production systems with exactly two outputs. This was also the case in our simulation results with StoNED. However, for production systems with more than two outputs, this conclusion is only valid for the order of the last two outputs (Henningsen et al. 2017). With regard to changing the order of other outputs, it cannot be guaranteed that identical estimations of frontier and/or efficiencies will result. Therefore, additional research is needed to investigate the impact of the order of outputs on the estimation results with StoNED for production systems with more than two outputs.

Moreover, our findings are subject to some limitations due to the design of the Monte Carlo simulation itself. For instance, since the estimations are still sometimes not very good, it could be analyzed how, e.g., a pseudolikelihood estimator instead of the method of moments change the results. Due to Andor and Hesse (2014) as well as Andor and Parmeter (2017) it can be expected that estimation performance will (on average) increase by using the pseudolikelihood estimator. [12] In addition, our insights are valid in general for the selected simulation design, here in

[12] However, this is only valid if the assumptions required for pseudolikelihood estimations are fulfilled. The method of moments is likely more robust to violations of these assumptions.

particular with respect to the representation of the technology as a translog function or logarithmized quadratic function, the number of DMUs, and the noise-to-signal ratio. Other potential influence factors would still have to be analyzed (see e.g. Andor and Hesse 2014). For instance, since two of our three functions are translog functions, the particularly good performance of SFA TL is not surprising. Additionally, the good estimations of SFA CD are understandable because a Cobb-Douglas function is the first order approximation to the translog function. Therefore, the comparison between the three methods in our simulation could be potentially biased in favor of the two SFA models. To analyze this aspect in more detail, additional functional forms should be added to the simulation design, especially those which do not correspond to the assumptions of the SFA models.

Acknowledgements The authors would like to express their gratitude to the editor and two anonymous reviewers for their constructive comments which contributed to the improvement of the paper. Additionally, the authors would like to thank Sebastian Gutgesell for his work on a former version of this paper.

Compliance with ethical standards

Conflict of interest The authors declare that they have no conflict of interest.

Ethical approval This article does not contain any studies with human participants or animals performed by any of the authors.

Informed consent Not applicable, since there are no individual participants included in the study.

6 Appendix

Tables 9–14

Table 9 Overview of the assessment criteria for all settings

	Frontier			Efficiency		
	MD	MSE	Rank (MSE)	MD	MSE	Rank (MSE)
StoNED	−0.0059	0.0094	2.17	−0.0050	0.0073	2.55
SFA CD	−0.0024	0.0076	1.93	−0.0041	0.0066	2.23
SFA TL	−0.0099	0.0088	1.72	−0.0101	0.0062	1.58
DEA CCR	−0.1954	0.0925	4.57	−0.1319	0.0505	4.62
DEA BCC	−0.0820	0.0492	4.10	−0.0522	0.0311	4.10

MD Mean deviation, *MSE* Mean squared error

Table 10 Overview of the assessment criteria for all settings without noise

	Frontier			Efficiency		
	MD	MSE	Rank (MSE)	MD	MSE	Rank (MSE)
StoNED	−0.0196	0.0027	2.67	−0.0166	0.0021	2.53
SFA CD	−0.0129	0.0030	2.67	−0.0111	0.0021	2.47
SFA TL	−0.0207	0.0023	1.47	−0.0178	0.0020	1.80
DEA CCR	−0.0500	0.0223	4.07	−0.0362	0.0139	4.00
DEA BCC	−0.0562	0.0057	4.13	−0.0508	0.0046	4.20

Table 11 Overview of the assessment criteria for all settings with noise

	Frontier			Efficiency		
	MD	MSE	Rank (MSE)	MD	MSE	Rank (MSE)
StoNED	−0.0180	0.0132	2.69	−0.0122	0.0091	2.33
SFA CD	−0.0011	0.0091	1.69	−0.0017	0.0081	2.16
SFA TL	−0.0063	0.0110	1.80	−0.0075	0.0076	1.51
DEA CCR	−0.2438	0.1159	4.73	−0.1638	0.0627	4.93
DEA BCC	−0.1318	0.0646	4.09	−0.0865	0.0399	4.07

MD Mean deviation, *MSE* Mean squared error

MD Mean deviation, *MSE* Mean squared error

Table 12 Variation of sample size in regard to mean absolute deviation and the efficiency

		Scenarios without noise			Scenarios with noise		
	Number of DMUs	TL CRS	TL DRS	Q	TL CRS	TL DRS	Q
StoNED	25	0.0533	0.0479	0.0462	0.0786	0.0789	0.0760
	50	0.0408	0.0363	0.0354	0.0759	0.0731	0.0734
	100	0.0306	0.0281	0.0265	0.0700	0.0703	0.0673
	200	0.0238	0.0229	0.0204	0.0659	0.0653	0.0636
	400	0.0191	0.0180	0.0150	0.0613	0.0609	0.0599
SFA CD	25	0.0474	0.0474	0.0474	0.0724	0.0737	0.0715
	50	0.0431	0.0426	0.0299	0.0715	0.0698	0.0697
	100	0.0376	0.0376	0.0220	0.0665	0.0681	0.0646
	200	0.0337	0.0348	0.0180	0.0641	0.0647	0.6019
	400	0.0321	0.0322	0.0153	0.0610	0.0609	0.0587
SFA TL	25	0.0544	0.0551	0.0554	0.0692	0.0705	0.0704
	50	0.0395	0.0386	0.0385	0.0692	0.0680	0.0691
	100	0.0265	0.0270	0.0258	0.0644	0.0656	0.0641
	200	0.0186	0.0197	0.0180	0.0620	0.0623	0.0617
	400	0.0143	0.0140	0.0124	0.0587	0.0588	0.0585
DEA CCR	25	0.0585	0.0958	0.0849	0.1209	0.1550	0.1456
	50	0.0428	0.1090	0.0902	0.1381	0.1860	0.1724
	100	0.0306	0.1234	0.0998	0.1630	0.2176	0.2019
	200	0.0213	0.1373	0.1098	0.1877	0.2498	0.2311
	400	0.0150	0.1540	0.1193	0.2123	0.2791	0.2593
DEA BCC	25	0.0804	0.0749	0.0779	0.1097	0.1132	0.1111
	50	0.0648	0.0584	0.0653	0.1198	0.1268	0.1228
	100	0.0498	0.0446	0.0528	0.1378	0.1460	0.1399
	200	0.0371	0.0330	0.0408	0.1582	0.1679	0.1604
	400	0.0273	0.0239	0.0310	0.1811	0.1919	0.1829

TL CRS Translog function with constant returns to scale, *TL DRS* Translog function with decreasing returns to scale, *Q* Logarithmized quadratic function

Table 13 Variation of noise-to-signal-ratio in regard to mean absolute deviation and the efficiency

		TL CRS		TL DRS		Q	
	Number of DMUs	Low	High	Low	High	Low	High
	$\rho_{nt\,s}$						
StoNED	0	0.0471	0.0245	0.0421	0.0230	0.0408	0.0206
	0.5	0.0545	0.0452	0.0536	0.0448	0.0521	0.0437
	1	0.0687	0.0616	0.0681	0.0616	0.0679	0.0607
	2	0.1085	0.0904	0.1063	0.0901	0.1040	0.0864
SFA CD	0	0.0453	0.0345	0.0450	0.0349	0.0353	0.0184
	0.5	0.0550	0.0483	0.0556	0.0483	0.0523	0.0437
	1	0.0674	0.0620	0.0669	0.0622	0.0670	0.0609
	2	0.0934	0.0813	0.0928	0.0833	0.0925	0.0806
SFA TL	0	0.0470	0.0198	0.0469	0.0202	0.0469	0.0187
	0.5	0.0558	0.0441	0.0566	0.0442	0.0562	0.0441
	1	0.0650	0.0610	0.0651	0.0607	0.0658	0.0607
	2	0.0867	0.0799	0.0861	0.0818	0.0873	0.0795
DEA CCR	0	0.0507	0.0223	0.1024	0.1370	0.0875	0.1096
	0.5	0.0597	0.0707	0.1147	0.1632	0.1011	0.1389
	1	0.1038	0.1612	0.1488	0.2218	0.1358	0.2039
	2	0.2249	0.3311	0.2480	0.3615	0.2401	0.3495
DEA BCC	0	0.0726	0.0381	0.0667	0.0339	0.0716	0.0415
	0.5	0.0707	0.0634	0.0664	0.0654	0.0674	0.0606
	1	0.0940	0.1331	0.0994	0.1426	0.0949	0.1342
	2	0.1795	0.2805	0.1942	0.2978	0.1887	0.2883

Low numbers of DMUs: Scenarios with 25 and 50 DMUs, High numbers of DMUs: Scenarios with 100, 200, and 400 DMUs

TL CRS Translog function with constant returns to scale, *TL DRS* Translog function with decreasing returns to scale, *Q* Logarithmized quadratic function, ρ_{nts} noise-to-signal ratio

Table 14 Variation of functional form in regard to mean absolute deviation and the efficiency

		Scenarios without noise		Scenarios with noise	
	Number of DMUs	Low	High	Low	High
StoNED	TL CRS	0.0471	0.0245	0.0773	0.0657
	TL DRS	0.0421	0.0230	0.0760	0.0655
	Q	0.0408	0.0206	0.0747	0.0636
SFA CD	TL CRS	0.0453	0.0345	0.0720	0.0639
	TL DRS	0.0450	0.0349	0.0718	0.0646
	Q	0.0353	0.0184	0.0706	0.0617
SFA TL	TL CRS	0.0470	0.0198	0.0692	0.0617
	TL DRS	0.0469	0.0202	0.0693	0.0622
	Q	0.0469	0.0187	0.0698	0.0615
DEA CCR	TL CRS	0.0507	0.0223	0.1295	0.1877
	TL DRS	0.1024	0.1370	0.1705	0.2488
	Q	0.0875	0.1096	0.1590	0.2308
DEA BCC	TL CRS	0.0726	0.0381	0.1147	0.1590
	TL DRS	0.0667	0.0339	0.1200	0.1686
	Q	0.0716	0.0415	0.1170	0.1611

Low numbers of DMUs: Scenarios with 25 and 50 DMUs, High numbers of DMUs: Scenarios with 100, 200, and 400 DMUs

TL CRS Translog function with constant returns to scale, *TL DRS* Translog function with decreasing returns to scale, *Q* Logarithmized quadratic function

References

Ahn H, Le MH (2015) DEA efficiency of German savings banks: evidence from a goal-oriented perspective. J Bus Econ 85:953–975

Aigner D, Lovell CA, Schmidt P (1977) Formulation and estimation of stochastic frontier production function models. J Econ 6:21–37

Andor M, Hesse F (2014) The StoNED age: the departure into a new era of efficiency analysis? A Monte Carlo comparison of StoNED and the "oldies" (SFA and DEA). J Prod Anal 41:85–109

Andor M, Parmeter C (2017) Pseudolikelihood estimation of the stochastic frontier model. Appl Econ 49:5651–5661

Badunenko O, Henderson DJ, Kumbhakar SC (2012) When, where and how to perform efficiency estimation. J R Stat Soc A Stat 175:863–892

Banker RD, Charnes A, Cooper WW (1984) Some models for estimating technical and scale inefficiencies in Data Envelopment Analysis. Manag Sci 30:1078–1092

Banker RD, Gadh VM, Gorr WL (1993) A Monte Carlo comparison of two production frontier estimation methods: corrected ordinary least squares and Data Envelopment Analysis. Eur J Oper Res 67:332–343

Battese GE, Coelli TJ (1988) Prediction of firm-level technical efficiencies with a generalized frontier production function and panel data. J Econ 38:387–399

Bogetoft P, Otto L (2011) Benchmarking with DEA, SFA, and R. Springer, New York, NY

Chambers RG, Chung Y, Färe R (1996) Benefit and distance functions. J Econ Theory 70:407–419

Chambers RG, Chung Y, Färe R (1998) Profit, directional distance functions, and Nerlovian efficiency. J Optim Theory Appl 98:351–364

Charnes A, Cooper WW, Rhodes E (1978) Measuring the efficiency of decision making units. Eur J Oper Res 2:429–444

Clermont M, Dirksen A, Dyckhoff H (2015) Returns to scale of Business Administration research in Germany. Scientometrics 103:583–614

Coelli T (1995) Estimators and hypothesis tests for a stochastic frontier function: a Monte Carlo analysis. J Prod Anal 6:247–268

Coelli T, Rao DSP, O'Donnel CJ, Battese GE (2005) An introduction to efficiency and productivity analysis. Springer, New York, NY

Färe R, Primont D (1995) Multi-output production and duality: Theory and applications. Kluwer, Boston

Gong BH, Sickles RC (1992) Finite sample evidence on the performance of stochastic frontiers and Data Envelopment Analysis using panel data. J Econ 51:259–284

Grosskopf S, Hayes KJ, Taylor LL, Weber WL (1997) Budget-constrained frontier measures of fiscal equality and efficiency in schooling. Rev Econ Stat 79:116–124

Hall P, Simar L (2002) Estimating a changepoint, boundary, or frontier in the presence of observation error. J Am Stat Assoc 97:523–534

Henningsen G, Henningsen A, Jensen U (2015) A Monte Carlo study on multiple output stochastic frontiers: a comparison of two approaches. J Prod Anal 44:309–320

Henningsen A, Bělín M, Henningsen G (2017) New insights into the stochastic ray production frontier. Econ Lett 156:18–21

Jensen U (2005) Misspecification preferred: the sensitivity of inefficiency rankings. J Prod Anal 23:223–244

Jewell RT (2017) Technical efficiency with multi-output, heterogeneous production: a latent class, distance function model of English football. J Prod Anal 48:37–50

Johnson AL, Kuosmanen T (2015) An introduction to CNLS and StoNED methods for efficiency analysis: Economic insights and computational aspects. In: Ray SC, Kumbhakar SC, Dua P (eds) Benchmarking for performance evaluation. Springer, New Delhi, 117–186

Jondrow J, Lovell CK, Materov IS, Schmidt P (1982) On the estimation of technical inefficiency in the stochastic frontier production function model. J Econ 19:233–238

Kumbhakar SC, Lovell CAK (2003) Stochastic Frontier Analysis. Cambridge University Press, Cambridge, UK

Kuosmanen T (2008) Representation theorem for convex nonparametric least squares. Econ J 11:308–325

Kuosmanen T (2012) Stochastic semi-nonparametric frontier estimation of electricity distribution networks: application of the StoNED method in the Finnish regulatory model. Energ Econ 34:2189–2199

Kuosmanen T, Johnson A (2017) Modeling joint production of multiple outputs in StoNED: Directional distance function approach. Eur J Oper Res 262:792–801

Kuosmanen T, Johnson A, Saastamoinen A (2015a) Stochastic nonparametric approach to efficiency analysis: a unified framework. In: Zhu J (ed) Data Envelopment Analysis: A Handbook of Models and Methods. Springer, Boston, 191–244

Kuosmanen T, Johnson A, Parmeter C (2015b) Orthogonality conditions for identification of joint production technologies: axiomatic nonparametric approach to the estimation of stochastic distance functions. Available at SSRN 2602340

Kuosmanen T, Kortelainen M (2012) Stochastic non-smooth envelopment of data: semi-parametric frontier estimation subject to shape constraints. J Prod Anal 38:11–28

Kuosmanen T, Saastamoinen A, Sipiläinen T (2013) What is the best practice for benchmark regulation of electricity distribution? Comparison of DEA, SFA and StoNED methods. Energ Policy 61:740–750

Lim E, Glynn PW (2012) Consistency of multidimensional convex regression. Oper Res 60:196–208

Löthgren M (1997) Generalized stochastic frontier production models. Econ Lett 57:255–259

Löthgren M (2000) Specification and estimation of stochastic multiple-output production and technical inefficiency. Appl Econ 32:1533–1540

Meeusen W, van den Broeck J (1977) Efficiency estimation from Cobb-Douglas production functions with composed error. Int Econ Rev 18:435–444

Olson JA, Schmidt P, Waldman DM (1980) A Monte Carlo study of estimators of stochastic frontier production functions. J Econ 13:67–82

Ondrich J, Ruggiero J (2001) Efficiency measurement in the stochastic frontier model. Eur J Oper Res 129:434–442

Pearson K (1896) Mathematical contributions to the theory of evolution III: regression. Hered Panmixia Philos T R Soc A 187:253–318

Perelman S, Santín D (2009) How to generate regularly behaved production data? A Monte Carlo experimentation on DEA scale efficiency measurement. Eur J Oper Res 199:303–310

Resti A (2000) Efficiency measurement for multi-product industries: a comparison of classic and recent techniques based on simulated data. Eur J Oper Res 121:559–578

Ruggiero J (1999) Efficiency estimation and error decomposition in the stochastic frontier model: a Monte Carlo analysis. Eur J Oper Res 115:555–563

Seijo E, Sen B (2011) Nonparametric least squares estimation of a multivariate convex regression function. Ann Stat 39:1633–1657

Shephard RW (1953) Cost and Production Functions. Princeton Univ, New Jersey

Shephard, R W (1970) Theory of cost and production functions. Princeton University Press, New Jersey

Spearman C (1904) General intelligence objectively determined and measured. Am J Psychol 15:201–293

Wooldridge JM (2013) Introductory Econometrics: A Modern Approach. South-Western, Mason